Acta Oceanol. Sin., 2019, Vol. 38, No. 8, P. 111–121
https://doi.org/10.1007/s13131-018-1274-5
http://www.hyxb.org.cn
E-mail: hyxbe@263.net

Spatial-temporal variations in net primary productivity in the Arctic from 2003 to 2016

Haili Li[1, 2], Changqing Ke[1, 2, 3*], Qinghui Zhu[4], Su Shu[1, 2]

[1] Jiangsu Provincial Key Laboratory of Geographic Information Science and Technology, Nanjing University, Nanjing 210023, China

[2] School of Geographic and Oceanographic Sciences, Nanjing University, Nanjing 210023, China

[3] Collaborative Innovation Center of Novel Software Technology and Industrialization, Nanjing 210023, China

[4] Navigation College, Dalian Maritime University, Dalian 116026, China

Received 26 March 2018; accepted 7 September 2018

Abstract

The area of Arctic sea ice has dramatically decreased, and the length of the open water season has increased; these patterns have been observed by satellite remote sensing since the 1970s. In this paper, we calculate the net primary productivity (NPP, calculated by carbon) from 2003 to 2016 based on sea ice concentration products, chlorophyll *a* (Chl *a*) concentration, photosynthetically active radiation (PAR), sea surface temperature (SST), and sunshine duration data. We then analyse the spatiotemporal changes in the Chl *a* concentration and NPP and further investigate the relations among NPP, the open water area, and the length of the open water season. The results indicate that (1) the Chl *a* concentration increased by 0.025 mg/m^3 per year; (2) the NPP increased by 4.29 mg/(m^2·d) per year, reaching a maximum of 525.74 mg/(m^2·d) in 2016; and (3) the Arctic open water area increased by 57.23×10^3 km^2/a, with a growth rate of 1.53 d/a for the length of the open water season. The annual NPP was significantly positively related to the open water area, the length of the open water season and the SST. The daily NPP was also found to have a lag correlation with the open water area, with a lag time of two months. With global warming, NPP has maintained an increasing trend, with the most significant increase occurring in the Kara Sea. In summary, this study provides a macroscopic understanding of the distribution of phytoplankton in the Arctic, which is valuable information for the evaluation and management of marine ecological environments.

Key words: sea ice, open water area, chlorophyll *a*, net primary productivity, Arctic

Citation: Li Haili, Ke Changqing, Zhu Qinghui, Shu Su. 2019. Spatial-temporal variations in net primary productivity in the Arctic from 2003 to 2016. Acta Oceanologica Sinica, 38(8): 111–121, doi: 10.1007/s13131-018-1274-5

1 Introduction

The extent of Arctic sea ice has rapidly declined in recent years (Cavalieri et al., 2003; Kinnard et al., 2006; Stroeve et al., 2007; Deng, 2014). The Fifth Assessment Report of the Intergovernmental Panel on Climate (IPCC) noted that the rate of the reduction in Arctic sea ice has reached (–48.0±3.0)×10^3 km^2/a (Eisenman et al., 2014), and the extent of multi-year ice decreased by nearly 30% from 2002 to 2010 (Ke et al., 2013). At the same time, the open water area has increased over a large range, and the length of the open water season has rapidly increased (Pabi et al., 2008; Arrigo and Van Dijken, 2011). These changes not only affect atmospheric and oceanic circulation in the Northern Hemisphere (Aagaard and Carmack, 1989) but also affect marine ecosystems (Ning et al., 1995; Rees, 2011; Kohlbach et al., 2016). Oceanic primary productivity, which is an important parameter used to describe marine ecosystems, has also increased, and a relatively strong correlation exists between the growing trend of oceanic primary productivity and the increasing trend of open water area (Arrigo and Van Dijken, 2011).

Scholars in China and other countries have conducted extensive relevant studies on oceanic primary productivity. Pabi et al. (2008) analysed the primary productivity of the Arctic Ocean from 1998 to 2006 and derived a mean primary productivity (calculated by carbon) for the entire Arctic of (419±33) Tg/a; the newly increased open water area resulted in relatively high annual productivity. Arrigo and Van Dijken (2011) found that the net primary productivity (NPP) of the total oceanic phytoplankton increased by 20% from 1998 to 2009 (in the range of 441–585 Tg/a), and the growth was most significant in the Kara Sea and Siberia Sea areas. Further analysis with a time series extending to 2012 indicated that the NPP rapidly increased in the Arctic Ocean, especially on the interior shelves in waters near the shelf break where the nutrient levels increased significantly (Arrigo and Van Dijken, 2015).

Using basic sea surface temperature (SST), salinity and primary productivity data acquired at observation stations, studies on the distribution characteristics of chlorophyll *a* (Chl *a*) concentrations and primary productivity in the Bering Sea indicated that the primary productivity of the continental shelf area was higher than that of the deep-sea area, and the mean primary productivity in the observation region was (0.50±0.23) mg/(m^3·h) (Liu et al., 2011). Le et al. (2014) analysed Chl *a* concentrations

Foundation item: The National Key Research and Development Program of China under contract No. 2016YFA0600102; the National Natural Science Foundation of China under contract No. 41371391; the Consulting Research Project of Chinese Academy of Engineering under contract No. 2016-XZ-15.

*Corresponding author, E-mail: kecq@nju.edu.cn

and primary productivity using data obtained from an *in situ* investigation in the Chukchi Sea and adjacent sea areas during the fifth Chinese Arctic Scientific Expedition. The results indicated that the peak Chl *a* concentrations and primary productivity values in 2012 appeared in the continental shelf area of the Chukchi Sea. Obvious regional features were observed due to the influence of factors such as nutritive salt.

With the drastic reduction in Arctic sea ice, the development of Arctic ship channels has been promoted, and the Arctic Research Expedition and commercial transportation have been further improved. The Arctic has abundant resources and enormous economic benefits and has gradually become the focus of the Arctic countries and even the key issue related to the future development of the world. China is increasing its cooperation with Arctic countries. The atmosphere and sea exchange, the ecological environment, sea ice changes, and resource development and utilization have become the focus of future research in the Arctic. Extensive development in this region will surely result in a series of ecological problems. Arctic ecology is fragile; once destroyed, its recovery would be very difficult. As an important parameter of marine ecosystems, studies on the spatiotemporal variations in the NPP and associated factors are helpful for understanding marine ecosystems and the characteristics of environmental change; moreover, such studies can provide data to support the monitoring and prediction of marine phytoplankton blooms and other phenomena and even provide decision support for ecological management (Zhou et al., 2003). At present, there is little knowledge of the large-scale NPP in the Arctic since most studies on oceanic primary productivity have been conducted in offshore areas; few studies have focused on Arctic primary productivity. These limited studies were mostly conducted in the Bering Sea and Chukchi Sea, and the data were collected during the Chinese Arctic Scientific Expedition. These data show the variations in elements over only a specific period in the summer, and a long-term series for the entire Arctic is lacking. Although remote sensing data accuracy is not as high as that of field observation data, a long-term dataset on the variation in the Arctic can be obtained only through a remote sensing approach.

The present study analyses the spatiotemporal variations in Chl *a* in the Arctic based on the National Ocean & Atmosphere Administration (NOAA) monthly mean SST reanalysis data from 2003 to 2016, monthly mean Chl *a* concentration and photosynthetically active radiation (PAR) data from MODIS (Aqua), and monthly mean sunshine duration data provided by the European Center for Medium-Range Weather Forecasts (ECMWF). We use remote sensing data to obtain NPP for the Arctic and analyse its spatiotemporal variation and use sea ice concentration data to obtain a long-term series of the variation in the open water area and the length of the open water season. We further investigate the relations among NPP, open water area, and length of the open water season in the Arctic.

2 Data and methods

2.1 *Study area*

In addition to polar regions within the Arctic Circle (66°34′–90°N), the study area in the Arctic also includes the marginal seas, inland seas, straits, and bays outside the Arctic Circle that are covered by sea ice (Deng, 2014). According to the division method of Cavalieri and Parkinson (2012), we divide the study area into nine sea areas (Fig. 1): Gulf of St. Lawrence, Baffin Bay/Labrador Sea, Hudson Bay, Greenland Sea, Kara and Barents Seas, Seas of Okhotsk and Japan, Bering Sea, Canadian Archipelago, and the Arctic Ocean.

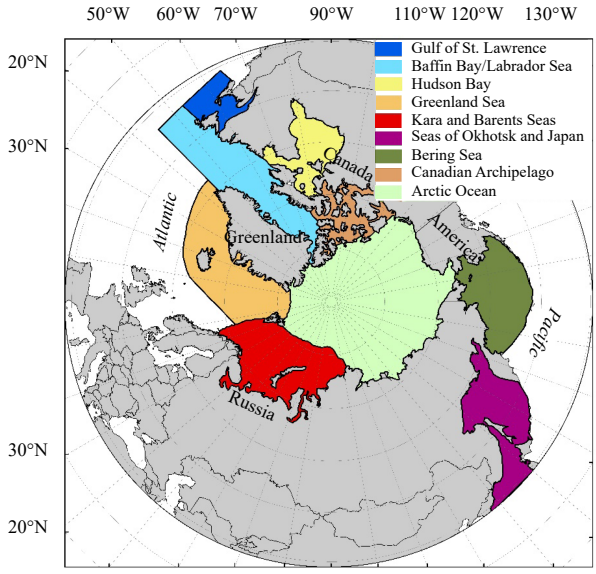

Fig. 1. Location map of the study area in the Arctic.

2.2 *Data*

2.2.1 *Chl a concentration and PAR*

Chl *a* concentration and PAR data are both acquired from MODIS (Aqua) level-III monthly mean data provided by the NASA's Ocean Color Processing Center (https://oceancolor.gsfc.nasa.gov). Further product information can also be found on this website. MODIS is one of the main sensors on the Terra and Aqua satellites. These two satellites coordinate with each other, and they can repeat observations of the entire earth surface every 1–2 d. The data were formally published in April 2000. The time covered by the MODIS/Aqua data is from July 4, 2002 to present. The Ocean Biological Processing Group (OBPG) completed all water colour reprocessing tasks for MODIS-Aqua water colour dataset in June 2015 (Meister and Franz, 2014). In this paper, we select the Chl *a* concentration and PAR data with a spatial resolution of 9 km×9 km from January 2003 to December 2016.

2.2.2 *SST*

The SST data are from the Optimum Interpolation Sea Surface Temperature V2 (OI.v2 SST) dataset provided by the Earth System Research Laboratory of NOAA (https://www.esrl.noaa.gov/psd/data/gridded/data.noaa.oisst.v2.html). The OI.v2 SST dataset includes the weekly, monthly, and monthly long-term mean data of the global SST, and the spatial resolution is 1°×1° (Reinart et al., 2001). The time series is from 1981 to present. Optimum Interpolation Sea Surface Temperature (OISST) analysis is produced weekly on a one-degree grid. This analysis uses *in situ* and satellite SSTs plus SSTs simulated by sea ice cover. The satellite SST data are adjusted for biases using the methods of Reynolds (1988) and Reynolds and Marsico (1993). The monthly NOAA OI.v2 SST product is obtained by a linear interpolation of the weekly OI data to obtain daily data and then averaging the daily values within a month (Maheshwari et al., 2013). The monthly and weekly mean SST data have the same format and spatial resolution. Compared to OISST, the OI.v2 SST analysis exhibits a modest improvement, especially at high latitudes (Reynolds et al., 2002). We select the monthly SST data from January 2003 to December 2016.

2.2.3 *Sunshine duration*

The sunshine duration data are from the ECMWF. ERA-Inter-

im is a reanalysis of the global atmosphere covering the data-rich period since 1979. It provides reanalysis data, such as surface net solar radiation, rainfall data, wind data and so on. The sunshine duration provided by ERA-Interim (http://apps.ecmwf.int/datasets/data/interim-mdfa/levtype=sfc/) is defined as the length of time when the solar radiation on the plane vertical to the direction of the sun is greater than or equal to 120 W/m^2 (https://software.ecmwf.int/wiki/display/TIGGE/Sunshine+duration). In this paper, we accumulate daily data to obtain monthly mean data. The principle is to acquire the daily mean by taking the mean of two periods from 0000 and 1200 UTC (Universal Time Coordinated) every day, thereby acquiring the monthly mean sunshine duration. The spatial resolution is 0.75°×0.75°. The unit is seconds, and it is divided by 3 600 to convert the unit to hours.

2.2.4 *Sea ice concentration*

The sea ice concentration refers to the percentage of the area accounted for by sea ice in a sea area (Comiso et al., 1997). The sea ice concentration data were provided by the United States National Snow and Ice Data Center (NSIDC) (http://nsidc.org/data/search) by adopting the NASA Team algorithm (Cavalieri et al., 1984; Swift and Cavalieri, 1985; Swift et al., 1985; Gloersen and Cavalieri, 1986). We select sea ice concentrations from product A (Nimbus-7 SMMR DMSP SSM/I-SSMIS passive microwave data) for the period from January 1982 to December 2014 and product B (near-real-time DMSP SSMIS daily polar gridded sea ice concentrations) for the period from January 2015 to December 2016. These products have spatial resolutions of 25 km×25 km, and the temporal resolution is divided into once every day and once every other day, with both being provided in a Tagged Image File Format (TIFF).

2.3 *Methods*

2.3.1 *Data preprocessing*

The sea ice concentration data are grey values, ranging from 0 to 255. A value of 255 represents no data, 254 represents a continent, 253 represents a continental contour or coastline, and 251 represents a data gap near the North Pole. We presume that the sea ice concentration near the North Pole is 100%. First, the continents and the continental contours are extracted, and then all remaining pixel values are divided by 251 to convert the grey values to 0%–100%, which is used to represent the sea ice concentration. Before we analyse the relationship between the area and length of open water season and the NPP, we transform all data in NC format to TIF format. All data are transformed to the North Pole azimuthal projection, which is the same projection used for the sea ice concentration, and are resampled to 25 km×25 km using the bilinear interpolation method. After these processes, the pixel locations of the different datasets are made consistent for further processing and analysis.

2.3.2 *Open water area and length of open water season*

Based on the definition of sea ice area, the open water area is calculated by summing the areas of the pixels where the sea ice concentration is less than or equal to 15%, which are calculated by multiplying the pixel area (25 km×25 km) by the concentration of open water (100% minus sea ice concentration). Because the data from December 3, 1987, to January 12, 1988, are missing, we use the data before and after this time period to interpolate the missing points.

We use the B (multi-year average maximum of open water area) minus the C (multi-year average minimum) to obtain the multi-year average amplitude A (i.e., A = B–C) between 1982 and 2016. The threshold equals C plus 50% of the A. Therefore, the date of sea ice retreat would be the date when open water first exceeded the threshold. Similarly, we define the date when open water first fell below the threshold as the date of sea ice advance (Arrigo and Van Dijken, 2011). We subtract the date of ice retreat from the date of sea ice advance to obtain the length of the open water season (Arrigo and Van Dijken, 2011; Li and Ke, 2017).

2.3.3 *Vertical generalized productivity mode*

Based on the normalized chlorophyll concentration, sunshine cycle, and optical depth, a light-dependent vertical generalized productivity mode (VGPM) was established to estimate the oceanic primary productivity (Behrenfeld and Falkowski, 1997). We use the VGPM to estimate the oceanic NPP, and the equation used is as follows:

$$NPP = 0.661\,25 \times P_{\mathrm{opt}}^{B} \times \frac{PAR}{PAR + 4.1} \times Z_{\mathrm{eu}} \times C_{\mathrm{hl}} \times dl, \quad (1)$$

where Z_{eu} represents the euphotic depth (Reinart et al., 2001; Li et al., 2009), and *NPP* represents the daily NPP from the surface to euphotic depth Z_{eu}. P_{opt}^{B} is the highest photosynthesis rate; *PAR* is the surface photosynthetically active radiation; C_{hl} is the Chl *a* concentration at the depth of the highest photosynthesis rate, which can be replaced with the surface Chl *a* concentration; and *dl* is the sunshine duration.

According to Eq. (1), the acquisition of *NPP* is related to five variables, and C_{hl} can be replaced with the surface Chl *a* concentration. The euphotic depth can be calculated with the method proposed by Morel and Berthon (1989), and its expression is described below.

$$Z_{\mathrm{eu}} = \begin{cases} 200.0 \times (C_{\mathrm{TOT}})^{-0.293} & (Z_{\mathrm{eu}} > 102)\,, \\ 568.2 \times (C_{\mathrm{TOT}})^{-0.746} & (Z_{\mathrm{eu}} \leqslant 102)\,, \end{cases} \quad (2)$$

where C_{TOT} is the euphotic Chl *a* concentration, and it is calculated as follows:

$$C_{\mathrm{TOT}} = \begin{cases} 40.2 \times (C_{\mathrm{hl}})^{0.507} & (C_{\mathrm{hl}} \geqslant 1.0)\,, \\ 38.0 \times (C_{\mathrm{hl}})^{0.425} & (C_{\mathrm{hl}} < 1.0)\,. \end{cases} \quad (3)$$

Equation (3) is the algorithm used by the VGPM to calculate the euphotic Chl *a* concentration, but this equation is from a model established for mid- and low-latitude sea areas. Based on the data from 309 stations in mid- and high-latitude sea areas, Morel and Berthon (1989) performed additional simulations to obtain the equation for C_{TOT} that is suitable for mid-high-latitude sea areas:

$$C_{\mathrm{TOT}} = 37.9 \times (C_{\mathrm{hl}})^{0.548}. \quad (4)$$

After calculating the euphotic Chl *a* concentration based on Eq. (4), we substitute the calculated result into Eq. (2) to compute the euphotic depth in the Arctic.

The empirical model that is most often used to estimate P_{opt}^{B} (Eppley, 1972; Yin et al., 2012) is based on its relation with temperature, and its expression is as follows:

$$P_{\mathrm{opt}}^{B} = \begin{cases} 1.13 & (T \leqslant -1.0)\,, \\ 4.00 & (T > 28.5)\,, \\ P_{\mathrm{opt}}^{B'} & (-1.0 < T \leqslant 28.5)\,, \end{cases} \quad (5)$$

where T is the sea surface temperature and $-1.0<T\leqslant 28.5$.

$$P_{\mathrm{opt}}^{B'}=1.295\,6+2.749\times10^{-1}\times T+6.17\times10^{-2}\times T^{2}-2.05\times10^{-2}\times T^{3}+2.462\times10^{-3}\times T^{4}-1.348\times10^{-4}\times T^{5}+3.413\,2\times10^{-6}\times T^{6}-3.27\times10^{-8}\times T^{7}. \quad (6)$$

3 Results

3.1 *Spatiotemporal variation in Chl a*

June is the month with the highest Chl *a* concentration in the Arctic. Therefore, we use the Chl *a* concentration data from June of each year to obtain Fig. 2. The black in the map indicates no data, which mainly resulted from sea ice cover or cloud cover. The large area of no data in the Arctic Ocean is mainly due to sea ice cover, so the sensor cannot obtain Chl *a* information under sea ice. Generally, the Chl *a* concentration is relatively low in the sea area far from land, and the concentration in this area is between 0 and 1.00 mg/m^3. The area with a Chl *a* concentration of less than 0.5 mg/m^3 in the Gulf of St. Lawrence is relatively large. The peak Chl *a* concentration appears in the marginal sea area, which is mostly the continental shelf region, and the maximum reached 94.00 mg/m^3 in 2016. As the time passes, the Chl *a* maximum increases. Because of cloud cover and other reasons, no Chl *a* data are observed in the southern parts of the Bering Sea (Fig. 2). The areas of the Greenland Sea and Baffin Bay/Labrador Sea with Chl *a* concentrations higher than 5 mg/m^3 increased significantly in June 2016. In June, the mean Chl *a* concentration in the Arctic generally exhibited an upward trend, reaching a maximum of 2.25 mg/m^3 in 2015.

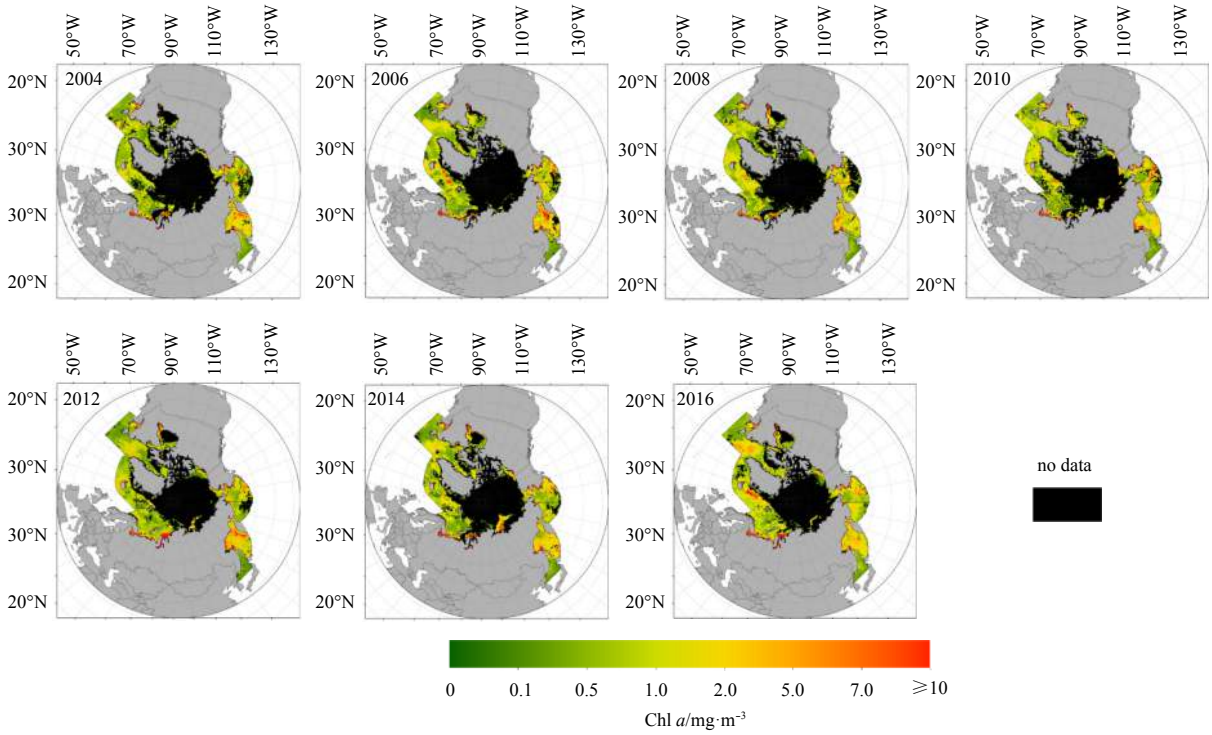

Fig. 2. Spatial distribution of Chl *a* in the Arctic in June every other year from 2004 to 2016.

The Arctic Chl *a* concentration fluctuates from year to year but exhibits a somewhat stable and slowly increasing trend, and the rate of increase is 0.025 mg/m^3 per year (Fig. 3). Due to the influence of the ambient environment, the variation in the Chl *a* concentrations in the different sea areas exhibits regional characteristics. Among all sea areas, the Chl *a* concentration is the highest in the Kara and Barents Seas, and the increasing trends are most obvious in these areas. The Chl *a* concentration is lowest in the Canadian Archipelago, where the variation is relatively gentle (Fig. 4).

3.2 *Net primary productivity*

The monthly mean NPP in the Arctic from 2003 to 2016 exhibits a rapid increase from February to April, and the rate of increase slows in May. The NPP reaches the annual maximum in June and then decreases from June to February of the following year, and the rate rapidly declines from July to October. The NPP reaches the annual minimum in February of the following year (Fig. 5).

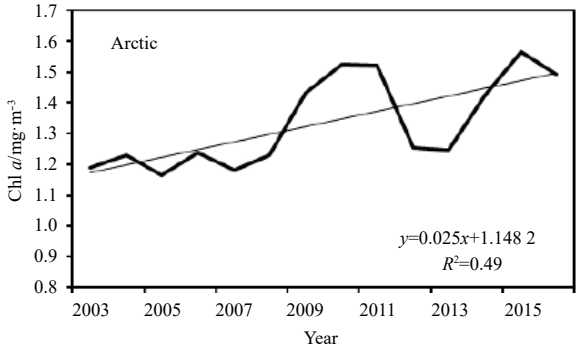

Fig. 3. Variation in the annual Chl *a* concentration in the Arctic from 2003 to 2016. *x* means year.

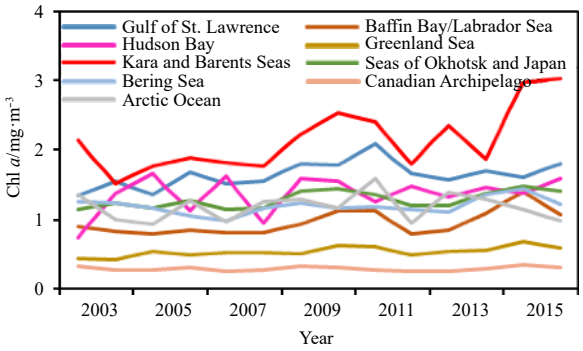

Fig. 4. Variation in the Chl *a* concentrations for the nine sea areas of the Arctic from 2003 to 2016.

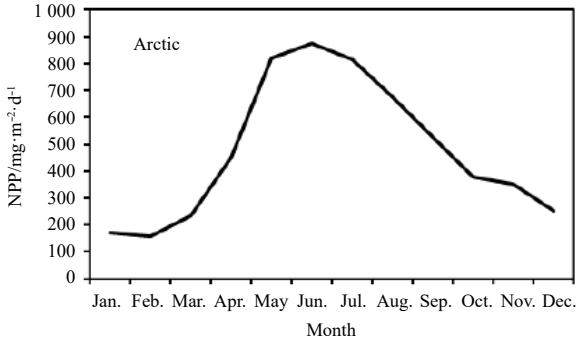

Fig. 5. Monthly averaged NPP in the Arctic.

We select the NPP in June 2004, 2006, 2008, 2010, 2012, 2014 and 2016 for the spatial distribution and trend analysis. The range of NPP range in the Arctic is relatively high and ranges from 0 to 1 000 mg/(m²·d), and the highest values are located in the region near the continent, such as the Obskaya Guba. With time, the region where NPP is between 500 and 2 000 mg/(m²·d) increases, and the region where NPP is between 0 and 500 mg/(m²·d) decreases in the Arctic. The region where NPP is below 500 mg/(m²·d) decreases, and the region where NPP is above 500 mg/(m²·d) increases in the Kara and Barents Seas, especially in 2016. The NPP in Baffin Bay/Labrador Sea mainly ranges from 0 to 500 mg/(m²·d) in June 2004, but in recent years, the region where NPP is between 700 and 2 000 mg/(m²·d) increased significantly (Fig. 6).

The inter-annual variability of the NPP fluctuated greatly, and it declined considerably in 2007 and 2012. The open water area increased in 2012, but the length of the open water season decreased. These changes may have an impact on the decrease in the NPP in 2012. The Arctic NPP generally exhibits an increasing trend, and it increases at a rate of 4.29 mg/(m²·d) per year on average (Fig. 7). The Arctic NPP reached its maximum in 2016, at 525.74 mg/(m²·d).

3.3 *Open water area and length of the open water season*

The open water area and the length of the open water season in the Arctic continued to increase from 2003 to 2016 (Fig. 8). The mean open water area is 12.9×10^6 km², and the mean length of the open water season is 160.14 d. The open water area is largest (2.47×10^6 km²) in the Greenland Sea and is smallest in the Canadian Archipelago (0.08×10^6 km²). The longest length (312.86 d) of the open water season is in the Gulf of St. Lawrence, and the shortest (62.93 d) is still in the Canadian Archipelago (Table 1). The open water area and the length of the open water season in the Arctic reached the maximums in 2016 (Fig. 8) at 13.52×10^6 km² and 182 d, respectively. The growth rates are 57.23×10^3 km²/a and 1.53 d/a, respectively. The largest contributions to the increasing open water area and the length of open water season occur in the Kara and Barents Seas, where the growth rates are 29.28×10^3 km²/a and 6.45 d/a, respectively, followed by the Arc-

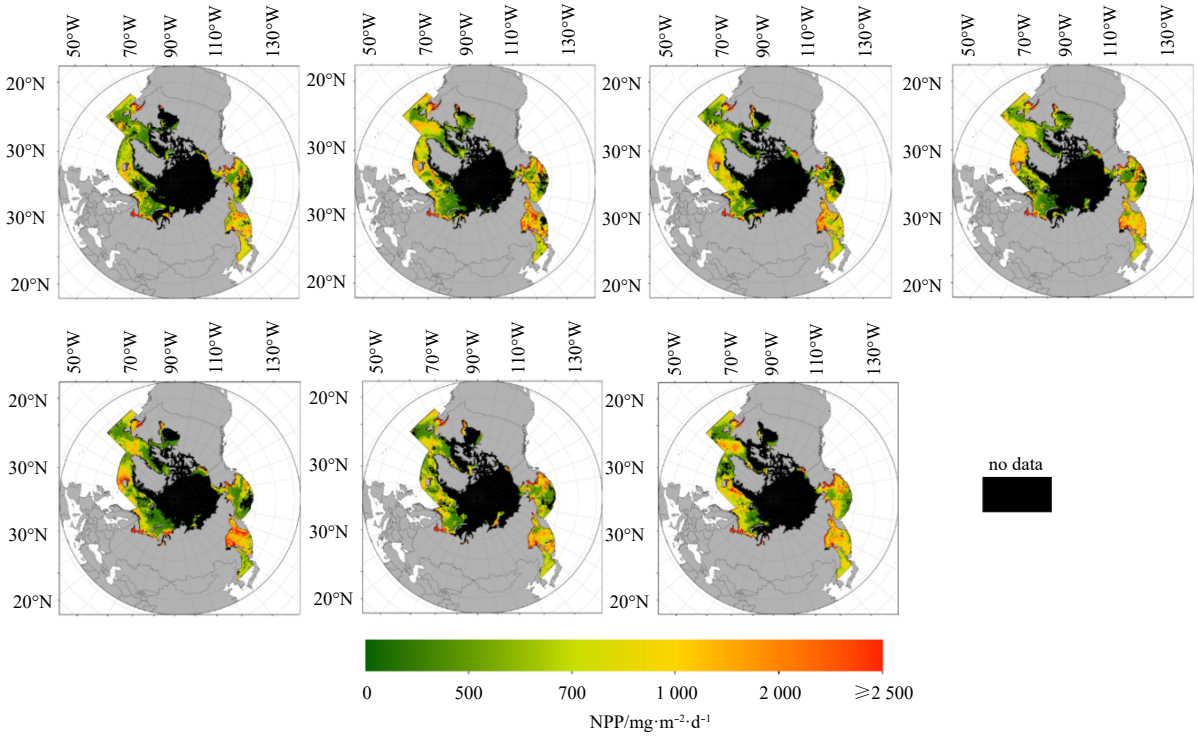

Fig. 6. Spatial distribution of the NPP in the Arctic in June every other year from 2004 to 2016.

tic Ocean, where the growth rates are 22.99×10³ km²/a and 2.18 d/a, respectively. Unlike the growing trends in the other eight sea areas, the open water area and the length of the open water season in Baffin Bay/Labrador Sea generally exhibit decreasing trends at –6.40×10³ km²/a and –1.89 d/a, respectively (Fig. 9). This result shows a general trend where the open water area or the length of the open water season increases in the Arctic; however, some spatial differences exist in the nine partitions of the Arctic.

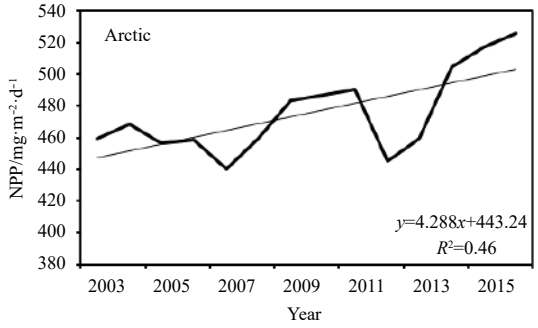

Fig. 7. Variation in the NPP in the Arctic from 2003 to 2016. *x* means year.

4 Discussion

4.1 *Relationship between the NPP and open water*

The NPP in the Arctic reaches a maximum (873.31 mg/(m²·d) in June and a minimum (158.49 mg/(m²·d)) in February (Fig. 10). The open water area begins to increase in March and reaches its peak in September. The lag correlation analysis of the NPP and open water area shows that when the open waters lag two months behind the NPP, the correlation coefficient is highest at

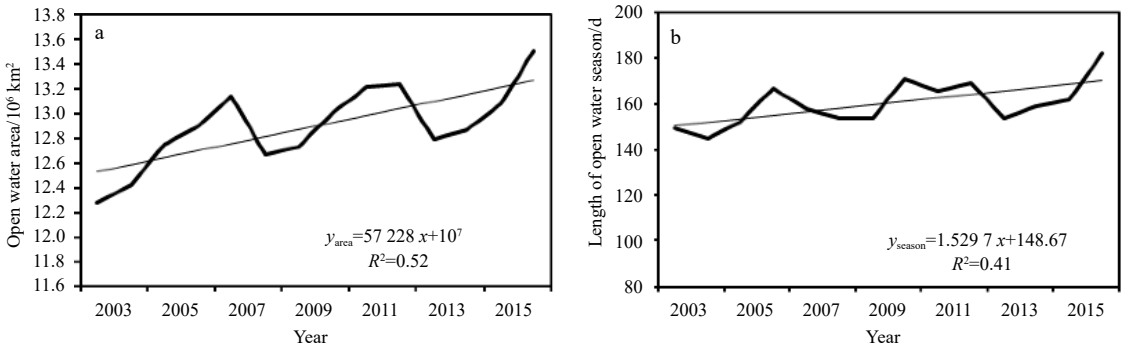

Fig. 8. Variations of open water area (a) and length of the open water season (b) for the Arctic from 2003 to 2016. *x* means year.

Table 1. The change of open water area (10^6 km^2) and length of the open water season (d) in the nine sea areas of the Arctic and entire Arctic from 2003 to 2016

	Open water area/10^6 km^2		Length of open water season/d	
	Mean	Standard deviation	Mean	Standard deviation
Gulf of St. Lawrence	0.83	0.02	312.86	31.80
Baffin Bay/Labrador Sea	2.39	0.06	194.57	18.14
Hudson Bay	0.53	0.04	153.21	8.95
Greenland Sea	2.47	0.04	174.14	36.12
Kara and Barents Seas	1.58	0.17	158.21	36.07
Seas of Okhotsk and Japan	2.31	0.04	275.93	16.84
Bering Sea	2.18	0.07	235.21	23.35
Canadian Archipelago	0.08	0.02	62.93	18.34
Arctic Ocean	0.72	0.16	91.07	13.41
Arctic	12.90	0.33	160.14	9.99

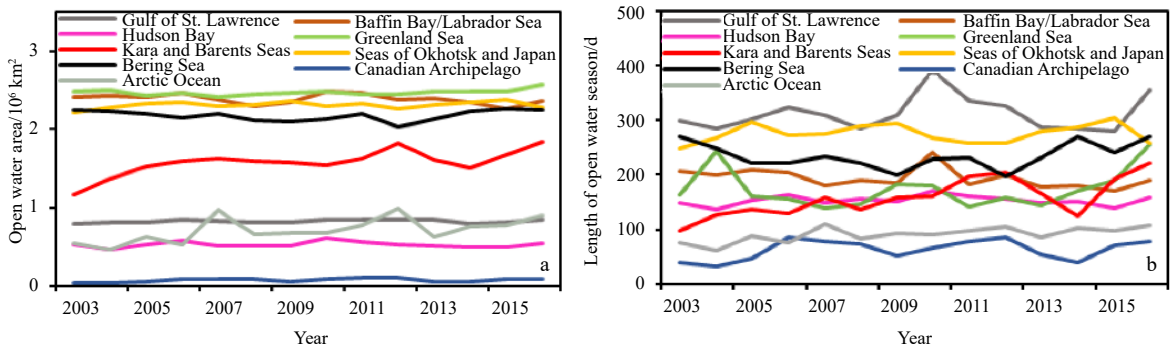

Fig. 9. Variations of open water area (a) and length of the open water season (b) for the nine sea areas of the Arctic from 2003 to 2016.

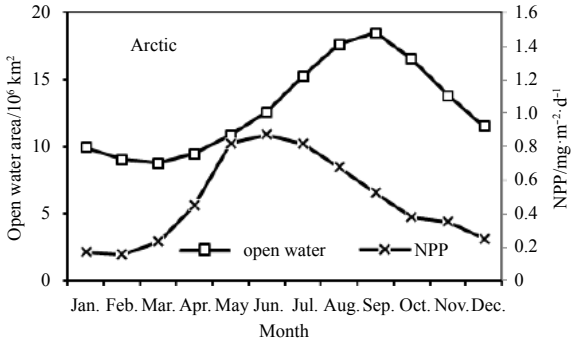

Fig. 10. Annual cycle of open water area and mean NPP from 2003 to 2016.

approximately 0.84. This result means that when NPP reaches its maximum, the open water area continues to increase. This pattern is probably due to the abundance of nutrients in the Arctic in February when the phytoplankton abundance begins to increase, which can affect the absorption of heat by the sea (Wang, 2011); then, the SST as well as the air temperature begins to rise. As a result, sea ice melts, and the open water area begins to increase. In June, the NPP reaches its maximum, and nutrients are consumed quickly. As the NPP begins to decrease, both the SST and the open water areas continue to increase. In the different sea areas, the time when the NPP reaches its peak value is concentrated in May, June or July. Except for the Bering Sea and Gulf of St. Lawrence, the time of the NPP peak in all sea areas is earlier than that for the open water area. In the Bering Sea, the Gulf of St. Lawrence, and the Seas of Okhotsk and Japan, the open water area does not exhibit an obvious peak, and the variation is gentle in the summer and fall seasons (Fig. 11). These sea areas are located at relatively low latitudes. The open water area is relatively extensive, and the changes in the summer and autumn are not considerable. The Hudson Bay, the Canadian Archipelago, and the Arctic Ocean are dominated by sea ice, and open water areas begin to appear in May. At the same time, the NPP appears in these three sea areas in March or April. In the other sea areas, a relatively high proportion of open water is present throughout the year.

The annual NPP per unit area in the Arctic is 173.66 g/(m²·a), and it is smallest in the Canadian Archipelago (45.82 g/(m²·a)), followed by that in the Arctic Ocean (84.41 g/(m²·a)) (Table 2). The annual NPP per unit area is greater than 100 g/(m²·a) in the other sea areas, and it is highest in the Gulf of St. Lawrence at 278.63 g/(m²·a). The total annual NPP of the entire Arctic is as high as 2 241.22 Tg/a. Because the total area is small, the total annual NPP is still lowest in the Canadian Archipelago at 3.52 Tg/a. Because of the low latitude, the total annual NPP is highest in the Seas of Okhotsk and Japan at 505.90 Tg/a.

In the Arctic, a significant positive correlation exists between the open water and total annual NPP (Fig. 12), but the correlations differ in various sea areas (Table 3). A significant positive correlation exists between the open waters of the Bering Sea and the annual NPP in the unit area because the Bering Sea is located at a relatively low latitude where the SST is relatively high, the open water area is relatively large and the length of the open water season is relatively long. The Chl *a* concentration and PAR are relatively high, and the annual NPP per unit area is maintained at a relatively high level. The overall variations in the open water area and the length of the open water season and the annual NPP per unit area are small and relatively stable from 2003 to 2016. Except for the Baffin Bay/the Labrador Sea and the Greenland Sea, where there is no significant relation between open water and the total annual NPP, the correlations are significant for the other sea areas (Table 3). This result indicates that the annual NPP variation in the Baffin Bay/Labrador Sea and the Greenland

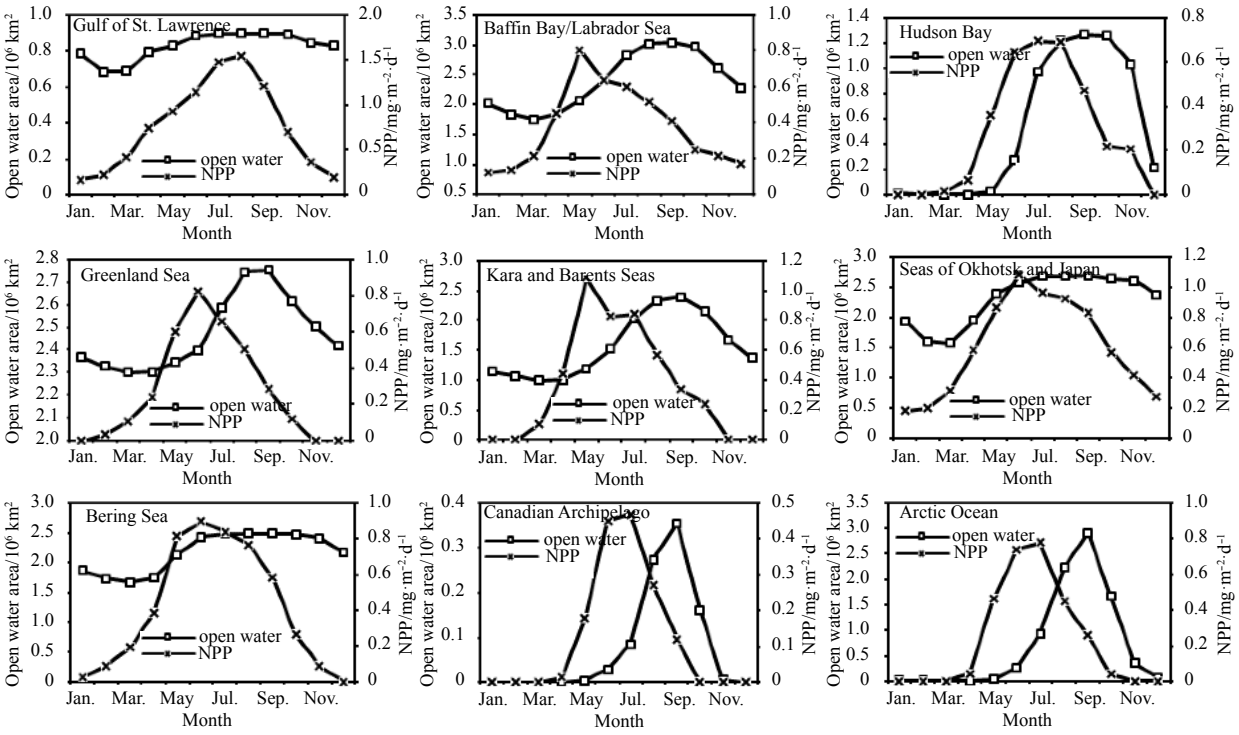

Fig. 11. Annual cycle of open water area and mean NPP for the nine sea areas of the Arctic from 2003 to 2016.

Sea does not have a considerable relation with the variation in open water area. The same result was obtained by Arrigo and Van Dijken (2011). We can speculate that the annual NPP variation is possibly dominated by other factors.

The variations in both open water areas and total annual NPP are roughly the same and generally exhibit increasing trends from 2003 to 2016 (Fig. 13). The open water area was relatively large in 2007, 2012, and 2016 (Fig. 13a), the length of the open water season was relatively long in 2006, 2010, 2012 and 2016 (Fig. 13b), and the total annual NPP was relatively high in 2006, 2011, and 2016. The open water area, the length of the open water seasons and the total annual NPP all reached a maximum in 2016. This result indicates that the increase in open water area or the length of the open water season can affect the NPP of phytoplankton and provide the appropriate living environments for the growth of phytoplankton. However, this result does not mean that when the open water area is increasing and the length of the open water season is long, the NPP should certainly increase. There must also be enough nutrients, Chl *a*, PAR, suitable temperatures and sufficient sunshine duration. In addition, there is a lag relationship between the NPP and open water area. When lag accumulation occurs, the times at which peak values occur will be interlaced. Therefore, the times when the open water and NPP reach their maximum values will not completely correspond.

In the previous part, it was mentioned that SST is a parameter that is often used to calculate the daily NPP, and it is an important factor that can affect the changes in Chl *a* concentration and NPP. Similar to the relationship between NPP and open wa-

Table 2. The annual NPP per unit area and total annual NPP in the nine sea areas of the Arctic and entire Arctic from 2003 to 2016

	Annual NPP per unit area/g·m^{-2}·a^{-1}		Total annual NPP/Tg·a^{-1}	
	Mean	Standard deviation	Mean	Standard deviation
Gulf of St. Lawrence	278.63	16.05	231.20	16.25
Baffin Bay/Labrador Sea	137.55	10.49	328.76	25.37
Hudson Bay	102.81	12.96	54.37	9.14
Greenland Sea	102.45	5.93	253.32	15.62
Kara and Barents Seas	135.51	22.27	214.49	48.95
Seas of Okhotsk and Japan	218.49	11.82	505.90	33.43
Bering Sea	150.54	15.32	328.31	42.38
Canadian Archipelago	45.82	6.13	3.52	1.18
Arctic Ocean	84.41	9.81	60.63	16.42
Arctic	173.66	9.70	2 241.22	159.24

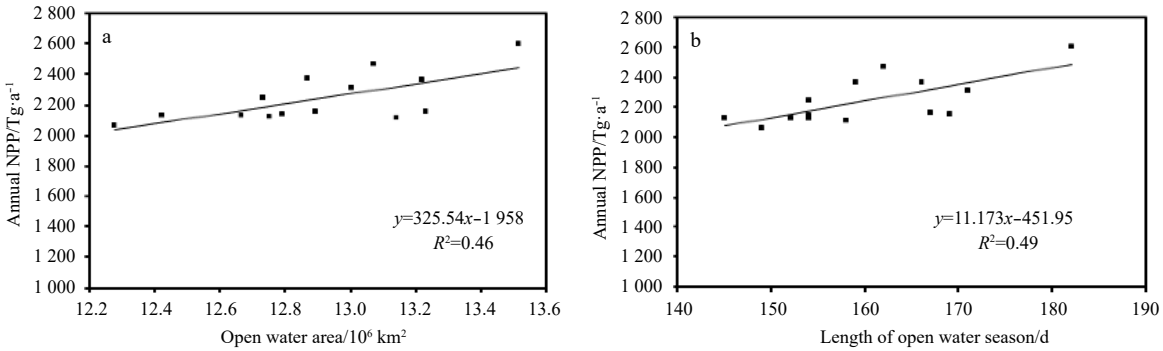

Fig. 12. Relationship between the total annual NPP and the open water area (a) and length of the open water season (b) in the Arctic from 2003 to 2016.

Table 3. Correlation coefficient between the annual NPP (annual NPP per unit area and total annual NPP) and open water in the nine sea areas of Arctic and the entire Arctic from 2003 to 2016

	Annual NPP per unit area		Total annual NPP	
	Open water area	Length of open water season	Open water area	Length of open water season
Gulf of St. Lawrence	0.41	0.42	0.67**	0.60*
Baffin Bay/Labrador Sea	–0.12	0.03	0.26	0.29
Hudson Bay	0.39	0.42	0.72**	0.72**
Greenland Sea	0.13	0.12	0.36	0.30
Kara and Barents Seas	0.25	0.46	0.65*	0.76**
Seas of Okhotsk and Japan	0.54*	0.36	0.72**	0.53*
Bering Sea	0.82**	0.84**	0.89**	0.87**
Canadian Archipelago	0.06	0.04	0.89**	0.85**
Arctic Ocean	0.19	0.32	0.88**	0.90**
Arctic	0.40	0.48	0.68**	0.70**

Note: $^{*}p$<0. 05; ** p<0.01.

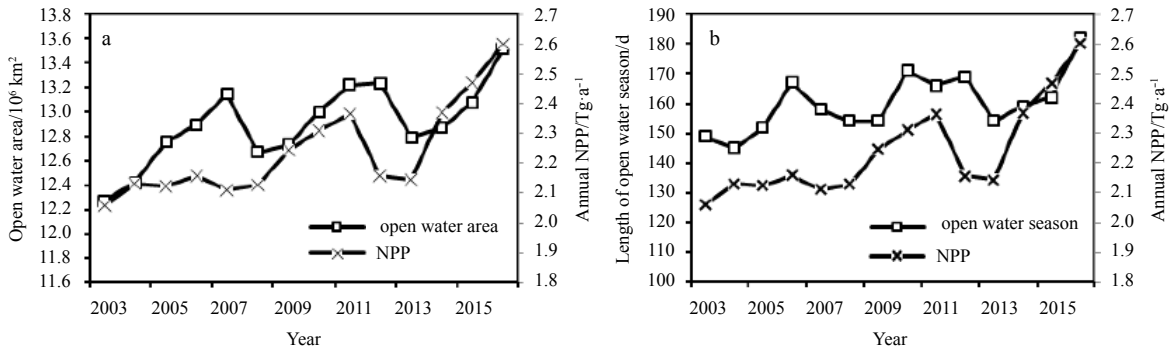

Fig. 13. Comparison of the total annual NPP with the mean open water area (a) and length of the open water season (b) in the Arctic from 2003 to 2016.

ter, a significant positive correlation exists between the SST and total annual NPP throughout the Arctic. In addition to the Baffin Bay/Labrador Sea and the Greenland Sea, the annual NPP variation in the Seas of Okhotsk and Japan did not have a considerable relation with the variation in SST (Table 4). This result indicates that SST is not a major factor driving the change in NPP in these seas. The areas that are mainly dominated by changes in SST are the Bering Sea and the Arctic Ocean. The results obtained by Li and Ke (2017) showed that the change in open water area lags behind the change in SST, and there is a high correlation between them. Thus, we speculate that with the increase in phytoplankton, photosynthesis produces more heat, the SST rises, the open water area increases, and finally, the NPP is impacted. This speculation also supports the finding that the times when both the open water and NPP reach their maximum values do not completely correspond.

Table 4. Correlation coefficient between the annual NPP (annual NPP per unit area and total annual NPP) and SST in the nine sea areas of Arctic and the entire Arctic from 2003 to 2016

	Annual NPP per unit area	Total annual NPP
Gulf of St. Lawrence	0.57*	0.58*
Baffin Bay/Labrador Sea	–0.20	0.09
Hudson Bay	0.56*	0.80**
Greenland Sea	0.00	0.15
Kara and Barents Seas	0.53	0.82**
Seas of Okhotsk and Japan	–0.09	–0.01
Bering Sea	0.91**	0.94**
Canadian Archipelago	0.48	0.60*
Arctic Ocean	0.31	0.87**
Arctic	0.41	0.56*

Note: * p<0. 05; ** p<0.01.

4.2 *Uncertainty of the NPP*

To verify the credibility of our result, we compare the NPP in the Greenland Sea to that found in other studies. The results obtained by Arrigo and Van Dijken (2015) showed that the total annual NPP in the Greenland Sea was 131.86 Tg/a from 2003 to 2012. Their study area included only the Greenland Sea within the Arctic Circle, whereas our study includes the sea area covered by sea ice outside the Arctic Circle. We recalculated the totally annual NPP for the Greenland Sea within the Arctic Circle during 2003–2012. The value in the present study is 124.17 Tg/a, which is slightly lower than that found in the previous study. The reason for this difference is that the open water area in this study is less than that in the study of Arrigo and Van Dijken (2015). The open water area in the previous study is mainly between 1.5×10^6 km^2 and 1.7×10^6 km^2, while the open water area in this study is mainly between 1.4×10^6 km^2 and 1.5×10^6 km^2. These two results are not considerably different, so we can conclude that the NPP results in this paper are reasonable.

Because the NPP estimates are the result of several remote sensing datasets, the uncertainty is also restricted by the uncertainty of the remote sensing products (Mélin et al., 2016; Tao et al., 2017). There are NPP gaps in some regions due to the lack of Chl *a* and PAR data. Chl *a* and PAR are both MODIS products, which are affected by cloud cover and precipitation (Fu et al., 2009). Most sea areas and some of the marginal sea in the Arctic Ocean do not have Chl *a* and PAR information due to sea ice cover. The most possible reason for the missing Chl *a* and PAR data in most of the marginal sea without sea ice is cloud cover. The SST is the result of optimal interpolation, and the accuracy is influenced by the coverage of the original data and the interpolation method. Sunshine duration is the result of a model based on the measured data, and the model result is lower than the true value. Therefore, the greatest impact on the NPP uncertainty stems from the missing data caused by cloud cover or other reasons and the data errors caused by the interpolation and modelling methods.

5 Conclusions

From 2003 to 2016, the spatial coverage of Chl *a* increased significantly, and the Chl *a* concentrations increased in all areas. The high Chl *a* concentrations are distributed throughout the sea margins of the study area, especially on the continental shelf, and low values are distributed in the Arctic Ocean or the sea areas near the Pacific and Atlantic. The Chl *a* concentration reaches a maximum in June of every year and declines to a minimum in February. The Chl *a* concentration is highest in the Kara and Barents Seas, which make the largest contributions to the increase in the Chl *a* concentration throughout the Arctic (with a rate of 0.07 mg/(m^3·a)). The NPP variation is similar to the variation in the Chl *a* concentration. The high daily NPP values are mainly distributed at the border between sea areas and the continent. The NPP increase is most obvious in the marginal region of the Kara and Barents Seas. From 2003 to 2016, the daily NPP in the Arctic exhibits an increasing trend, which reaches its maximum in 2016.

From 2003 to 2016, the open water area and the length of the open water season generally exhibited increasing trends. The

changes in the Kara and Barents Seas and the Arctic Ocean make large contributions to the growth in the open water area and the length of the open water season in the Arctic. There is a lag relationship between the daily NPP and open water area (two months). Significantly positive correlations exist between the total annual NPP and the open water area, the length of the open water season, and the SST in the Arctic. Except for the Greenland Sea and Baffin Bay/Labrador Sea, the total annual NPP of the other sea areas is significantly positively correlated with the open water area and the length of the open water season. The open water area, the length of the open water season, and the total annual NPP all peaked in 2016. The open water area increased and the length of the open water season became longer, creating a favourable environment for the increase in NPP. It should also be noted that increases in NPP also require adequate levels of nutrients, SST, Chl *a*, sunshine, PAR, and so on. Abundant nutrients and sunlight, suitable temperatures and high Chl *a* concentrations provide favourable conditions for the growth of phytoplankton, resulting in high NPP. These factors must work together to produce NPP, and all of them are indispensable.

Factors that affect NPP are complicated and diverse, and some influencing factors (e.g., nutritive salts) are not considered because of data availability. As remote sensing techniques develop, the remote sensing data will become more accurate. As the Arctic expeditions continue to advance, more field measurement data will be obtained for validation, and more accurate results for the studies of Arctic NPP will be obtained. In future work, we will focus on typical sea areas in the Arctic (such as the Kara and Barents Seas or the Bering Sea, where the changes are relatively obvious), analyse the spatiotemporal variation in the NPP and the relationship between the NPP and open water area, the length of the open water season. Moreover, we will more deeply investigate the internal driving mechanism of NPP changes.

Acknowledgements

We thank the National Snow and Ice Data Center for the sea ice concentration data, NASA ocean colour for the chlorophyll *a* concentration and PAR data, NOAA for the SST data and ECMWF for the sunshine duration data.

References

Aagaard K, Carmack E C. 1989. The role of sea ice and other fresh water in the Arctic circulation. Journal of Geophysical Research: Oceans, 94(C10): 14485–14498, doi: 10.1029/JC094iC10p14485

Arrigo K R, Van Dijken G L. 2011. Secular trends in Arctic Ocean net primary production. Journal of Geophysical Research: Oceans, 116(C9): C09011

Arrigo K R, Van Dijken G L. 2015. Continued increases in Arctic Ocean primary production. Progress in Oceanography, 136: 60–70, doi: 10.1016/j.pocean.2015.05.002

Behrenfeld M J, Falkowski P G. 1997. Photosynthetic rates derived from satellite-based chlorophyll concentration. Limnology and Oceanography, 42(1): 1–20, doi: 10.4319/lo.1997.42.1.0001

Cavalieri D J, Gloersen P, Campbell W J. 1984. Determination of sea ice parameters with the Nimbus 7 SMMR. Journal of Geophysical Research: Atmospheres, 89(D4): 5355–5369, doi: 10.1029/JD089iD04p05355

Cavalieri D J, Parkinson C L. 2012. Arctic sea ice variability and trends, 1979–2010. The Cryosphere, 6(4): 881–889, doi: 10.5194/tc-6-881-2012

Cavalieri D J, Parkinson C L, Vinnikov K Y. 2003. 30-year satellite record reveals contrasting Arctic and Antarctic decadal sea ice variability. Geophysical Research Letters, 30(18): 1970

Comiso J C, Cavalieri D J, Parkinson C L, et al. 1997. Passive microwave algorithms for sea ice concentration: A comparison of two techniques. Remote Sensing of Environment, 60(3): 357–384, doi: 10.1016/S0034-4257(96)00220-9

Deng Juan. 2014. Northern Hemisphere sea ice variability and its relationship with climate factors (in Chinese) [dissertation]. Nanjing: Nanjing University

Eisenman I, Meier W N, Norris J R. 2014. Spurious jump in the satellite record: is Antarctic sea ice really expanding?. The Cryosphere Discussions, 8(1): 273–288, doi: 10.5194/tcd-8-273-2014

Eppley R W. 1972. Temperature and phytoplankton growth in the sea. Fishery Bulletin, 70(4): 1063–1085

Fu Dongyang, Pan Delu, Ding Youzhuan, et al. 2009. Quantitative study of effects of the sea chlorophyll-a concentration by typhoon based on remote-sensing. Haiyang Xuebao (in Chinese), 31(3): 46–56

Gloersen P, Cavalieri D J. 1986. Reduction of weather effects in the calculation of sea ice concentration from microwave radiances. Journal of Geophysical Research: Oceans, 91(C3): 3913–3919, doi: 10.1029/JC091iC03p03913

Ke Changqing, Peng Haitao, Sun Bo, et al. 2013. Spatio-temporal variability of Arctic sea ice from 2002 to 2011. Journal of Remote Sensing (in Chinese), 17(2): 452–466

Kinnard C, Zdanowicz C M, Fisher D A, et al. 2006. Climatic analysis of sea-ice variability in the Canadian Arctic from operational charts, 1980–2004. Annals of Glaciology, 44(1): 391–402

Kohlbach D, Graeve M, Lange B A, et al. 2016. The importance of ice algae-produced carbon in the central Arctic Ocean ecosystem: Food web relationships revealed by lipid and stable isotope analyses. Limnology and Oceanography, 61(6): 2027–2044, doi: 10.1002/lno.10351

Le Fengfeng, Hao Qiang, Jin Haiyan, et al. 2014. Size structure of standing stock and primary production of phytoplankton in the Chukchi Sea and the adjacent sea area during the summer of 2012. Haiyang Xuebao (in Chinese), 36(10): 103–115

Li Yunliang, Zhang Yunlin, Liu Mingliang. 2009. Calculation and retrieval of euphotic depth of Lake Taihu by remote sensing. Journal of Lake Sciences (in Chinese), 21(2): 165–172, doi: 10.18307/2009.0203

Li Haili, Ke Changqing. 2017. Open water variability in the North Pole from 1982 to 2016. Haiyang Xuebao (in Chinese), 39(12): 109–121

Liu Zilin, Chen Jianfang, Liu Yanlan, et al. 2011. The size-fractionated chlorophyll a concentration and primary productivity in the Bering Sea in the summer of 2008. Haiyang Xuebao (in Chinese), 33(3): 148–157

Mélin F, Sclep G, Jackson T, et al. 2016. Uncertainty estimates of remote sensing reflectance derived from comparison of ocean color satellite data sets. Remote Sensing of Environment, 177: 107–124, doi: 10.1016/j.rse.2016.02.014

Maheshwari M, Singh R K, Oza S R, et al. 2013. An investigation of the southern ocean surface temperature variability using long-term optimum interpolation SST data. ISRN Oceanography, 2013: 392632

Meister G, Franz B A. 2014. Corrections to the MODIS Aqua calibration derived from MODIS Aqua ocean color products. IEEE Transactions on Geoscience and Remote Sensing, 52(10): 6534–6541, doi: 10.1109/TGRS.2013.2297233

Morel A, Berthon J F. 1989. Surface pigments, algal biomass profiles, and potential production of the euphotic layer: relationships reinvestigated in view of remote-sensing applications. Limnology and Oceanography, 34(8): 1545–1562, doi: 10.4319/lo.1989.34.8.1545

Ning Xiuren, Liu Zilin, Shi Junxian. 1995. Assessment of primary productivity and potential fishery production in the Bohai Sea, Yellow Sea and East China Sea. Haiyang Xuebao (in Chinese), 17(3): 72–84

Pabi S, Van Dijken G L, Arrigo K R. 2008. Primary production in the Arctic Ocean, 1998–2006. Journal of Geophysical Research: Oceans, 113(C8): C08005

Rees G W. 2011. Remote Sensing of Snow and Ice (in Chinese). Che Tao, Gao Feng, trans. Zhengzhou: Yellow River Conservancy Press

Reinart A, Arst H, Erm A, et al. 2001. Optical and biological properties of Lake Ülemiste, a water reservoir of the city of Tallinn II: Light climate in Lake Ülemiste. Lakes and Reservoirs Research and Management, 6(1): 75–84, doi: 10.1046/j.1440-1770.2001.00128.x

Reynolds R W. 1988. A real-time global sea surface temperature analysis. Journal of Climate, 1(1): 75–87, doi: 10.1175/1520-0442(1988)001<0075:ARTGSS>2.0.CO;2

Reynolds R W, Marsico D C. 1993. An improved real-time global sea surface temperature analysis. Journal of Climate, 6(1): 114–119, doi: 10.1175/1520-0442(1993)006<0114:AIRTGS>2.0.CO;2

Reynolds R W, Rayner N A, Smith T M, et al. 2002. An improved in situ and satellite SST analysis for climate. Journal of Climate, 15(13): 1609–1625, doi: 10.1175/1520-0442(2002)015<1609:AIISAS>2.0.CO;2

Stroeve J, Holland M M, Meier W, et al. 2007. Arctic sea ice decline: faster than forecast. Geophysical Research Letters, 34(9): L09501

Swift C T, Fedor L S, Ramseier R O. 1985. An algorithm to measure sea ice concentration with microwave radiometers. Journal of Geophysical Research: Oceans, 90(C1): 1087–1099, doi: 10.1029/JC090iC01p01087

Swift C T, Cavalieri D J. 1985. Passive microwave remote sensing for sea ice research. EOS, 66(49): 1210–1212, doi: 10.1029/EO066i049p01210

Tao Zui, Ma Sheng, Yang Xiaofeng, et al. 2017. Assessing the uncertainties of phytoplankton absorption-based model estimates of marine net primary productivity. Acta Oceanologica Sinica, 36(6): 112–121, doi: 10.1007/s13131-017-1047-8

Wang Weibo. 2011. Solar radiation observation and bio-optical properties of seawater in Canada Basin (in Chinese) [dissertation]. Qingdao: Ocean University of China

Yin Yan, Zhang Yunlin, Shi Zhiqiang, et al. 2012. Estimation of spatial and seasonal changes in phytoplankton primary production in Meiliang Bay, Lake Taihu, based on the vertically generalized production model and MODIS data. Acta Ecologica Sinica (in Chinese), 32(11): 3528–3537, doi: 10.5846/stxb

Zhou Weihua, Huo Wenyi, Yuan Xiangcheng, et al. 2003. Distribution features of chlorophyll a and primary productivity in high frequency area of red tide in East China Sea during Spring. Chinese Journal of Applied Ecology (in Chinese), 14(7): 1055–1059